Association Behavior of PDMA-*g*-PMMA in Mixed Solvents and Its Application as a DNA Separation Medium

Jun Zhang, Yanmei Wang, Dehai Liang, Qicong Ying, and Benjamin Chu*

Department of Chemistry, Stony Brook University, Stony Brook, New York 11794-3400

Received May 18, 2004; Revised Manuscript Received October 14, 2004

ABSTRACT: PDMA-*g*-PMMA (poly(*N*,*N*-dimethylacrylamide)-*graft*-poly(methyl methacrylate)) graft copolymers were synthesized by radical copolymerization of DMA (*N*,*N*-dimethylacrylamide) and vinyl-PMMA macromonomers with AIBN (2,2′-azobis(isobutyronitrile)) as an initiator. The association behavior of high molecular weight graft copolymers of PDMA-*g*-PMMA with low graft density in methanol−TBE (tris(hydroxymethyl)aminomethane−boric acid−EDTA) buffer solvent mixtures has been investigated by laser light scattering. With changing solvent quality, the PMMA side chains could be associated. The association points acted as cross-linking points which effectively increased the molecular weight of the associated graft copolymers and also prevented the entangled backbone chains from sliding away against one another. This association behavior could be used to improve the quasi-network formation of such copolymers as better separation media in DNA capillary electrophoresis. pBR322/Hae III digest was successfully separated within 10 min in a 10 cm long capillary with one base pair (bp) resolution (123/124 bp). The methanol component in the solvent mixture affected not only the polymer conformation in solution but also the DNA conformation. The average hydrodynamic radius of DNA decreased from 76.2 nm in 1×TBE buffer to 43.7 nm in 30% methanol + 70% 1×TBE (volume fraction) mixed solvent, resulting in a corresponding change in electrophoretic mobility.

Introduction

Amphiphilic block and graft copolymers consisting of hydrophilic and hydrophobic parts have attracted much attention due to their versatile applications.[1−3] Extensive studies showed that block and graft copolymers could form micelles or aggregates in solution if one part of the copolymer was soluble while the other part insoluble in the solvent.[4,5] Micellization and aggregation behaviors of block and graft copolymers have been investigated experimentally and theoretically.[6,7] Generally, the block copolymer forms micelles with a core−shell structure having the insoluble block as the core and the soluble block as the swollen shell. On the other hand, graft copolymers have more flexibility to form a variety of structures based on the solvent quality. The associated chains could be backbone chains or side chains depending on their solubility in a given solvent.[8] Compared with block copolymers, graft copolymers could form micelles with less number of chains. Even unimolecular micelles could often be formed by intramolecular association. In a graft copolymer, one main chain may consist of many side chains while diblock (or triblock) copolymers have only one (or two) associative chain segment(s).[9] The combination of intra- and intermolecular association offers the graft copolymers a more flexible ability to form diverse structures that can be used in many applications. It is one of the objectives of this article to demonstrate the utility of such graft copolymers as effective separation media in capillary electrophoresis (CE).

Capillary electrophoresis using polymer solutions as separation media has been proven to be a powerful method to separate charged macromolecules of biological and medical interests.[10−13] One of the key components in controlling the efficiency of capillary electrophoresis is the separation medium. An ideal separation medium for DNA separations using capillary electrophoresis should possess the following properties: high sieving ability, dynamic coating ability, and relatively low viscosity. With these three simultaneous specifications, the separation medium can be used to facilitate the automation of CE and to further enhance its performance. For a given homopolymer, it has been difficult to optimize the three desired specifications. Aiming at this goal, a range of new copolymers become better alternatives to homopolymers, including PAM-*co*-PDMA random copolymer,[14] PNIPAM-*g*-PEO[15] and PAM-*g*-PNIPAM[16] graft copolymers, block copolymers,[2,17,18] and PVP-*i*-PDMA quasi-interpenetrating networks.[19] All of these materials alleviate the polymer immiscibility and greatly enhance the DNA separation resolution and throughput.

A polymer solution as a good separation medium requires that a network above its overlap concentration would be formed with a certain effective pore size through which the DNA fragments have to migrate.[20] DNA fragments could be separated in size by using a chemically cross-linked sieving matrix. On the basis of this mechanism, graft copolymer solutions should have a better separation performance than those of linear polymer solutions. The reason is when the DNA fragment has a size larger than the pore size formed by using linear polymer solution, the network would adjust itself to enlarge the mesh size by sliding away the entangled chains from one another, a movement which is detrimental to the resolution.[21] While in a polymer network formed by entanglements of graft copolymer chains, the cross-linking points would be less mobile due to side chain obstructions or associations. The decrease in the slippage of those entanglements stabilizes the mesh formation and therefore enhances the resolution. Furthermore, the association could effectively increase the polymer molecular weight to a range beyond the synthetic limits.

* Corresponding author: Tel +631-632-7928; Fax +631-632-6518; e-mail bchu@notes.cc.sunysb.edu.

10.1021/ma0490193 CCC: $30.25 © 2005 American Chemical Society
Published on Web 02/03/2005

Table 1. Characteristics of Graft Copolymers PDMA-*g*-PMMA

sample	1	2	3
feed ratio			
vinyl-PMMA (g)	0.020	0.025	0.005
DMA (g)	7.20	3.60	7.20
AIBN (mg)	0.2957	0.2957	0.2957
total M_w[a] (g/mol)	3.33×10^6	2.37×10^6	2.38×10^6
mol wt distribution[b]	2.1	2.2	2.0
graft chain weight fraction[c]	0.021	0.02	0.007
graft density[c] (av side chain no. per molecule)	14.0	9.4	3.4

[a] Static light scattering in methanol solution. [b] Estimated from dynamic light scattering. [c] ^{1}H NMR spectroscopy for D_2O solution.

Itakura et al. designed and synthesized a graft copolymer with the side chains as the association points.[22] The association behavior was not controlled by temperature but by solvent quality. In this work, poly(*N,N*-dimethylacrylamide)-*graft*-poly(methyl methacrylate) (PDMA-*g*-PMMA) was synthesized. The reason we have chosen PDMA as the backbone is that PDMA has both good sieving ability and dynamic coating ability for DNA separation. The graft copolymer was fully soluble in pure methanol solvent. By adding water to the methanol solution, the solvent quality became worse for the grafted PMMA side chains, and hence association was induced. Compared with the graft copolymer synthesized by Itakura et al., our copolymer has a higher molecular weight and a lower grafting density which should come closer to meet the requirements for DNA separation. The purpose of the present work is to investigate how the association behavior of PMDA-*g*-PMMA in mixed solvent of methanol/water could improve the performance on dsDNA separations by capillary electrophoresis. The results could then provide us with the rationale on how self-assembled polymers in solution could be used as effective separation media.

Experimental Section

Materials. *N,N*-Dimethylacrylamide (DMA) was purchased from Polysciences, Inc. (Warrington, PA), and was fractionally distilled under vacuum before polymerization. Macromonomer (vinyl-PMMA) ($M_w = 5000$, $M_n = 4700$) which had a styrene group at one terminal was obtained from Polymer Source, Inc. (Québec, Canada), and used without further purification. Graft copolymers of PDMA-*g*-PMMA were synthesized by radical copolymerization of DMA and vinyl-PMMA with 2,2′-azobis(isobutyronitrile) (AIBN) as an initiator. AIBN was recrystallized twice in methanol. The solvent, dioxane, was freshly and fractionally distilled before use. A solution of DMA (3.60 g), PMMA macromonomer (0.025 g), AIBN (0.3 mg), and dioxane (3.42 mL) was placed in a three-neck round-bottom flask. High-purity nitrogen was bubbled into the solution for 1 h to remove oxygen. The copolymerization process was carried out at 53 °C for 16 h. The solution after the polymerization became gellike, was diluted by chloroform, and followed by precipitation with hexane. The obtained polymer was dried under vacuum. Table 1 summarizes the characteristics of the graft copolymers—molecular weight, molecular weight distribution (MWD), side chains weight fraction, and graft density. All polymers were tested as the separation media and showed comparable sieving ability. Sample 2 was chosen to investigate the solution behavior.

pCMVβ plasmid DNA (7164 bp) encoding β-galactosidase (Clontech, Palo Alto, CA) was extracted from cultured *E. coli* utilizing a Qiagen (Valencia, CA) GigaPrep DNA isolation kit.

Laser Light Scattering Measurements. The stock solution was prepared by dissolving the graft copolymer in methanol which was first dried by 4 Å molecular sieves and freshly distilled before use. Methanol was added to the stock solution to give the desired concentration. 1×TBE was also added in order to make the graft copolymer forming aggregates in the mixed solvent. To prepare dust-free solutions for light scattering measurements, the solutions were filtered through Millipore sterile membrane filters (0.22 μm pore size) directly into light scattering cells, which had been rinsed with distilled acetone to ensure a dust-free condition before use.

We used a standard laboratory-built laser light scattering (LLS) instrument equipped with a BI-9000 AT digital correlator and a solid-state laser (DPSS, Coherent, 200 mW, 532 nm) to perform the LLS studies. For the static LLS measurements, the angular dependence of the excess absolute time-averaged scattered intensity, known as the Rayleigh ratio $R_{vv}(\theta)$, was measured. In the dilute solution limit, the reciprocal of $R_{vv}(\theta)$ follows the relationship

$$\frac{HC}{R_{vv}(\theta)} \approx \frac{1}{M_w}\left(1 + \frac{\langle R_g\rangle^2 q^2}{3}\right) + 2A_2C \tag{1}$$

where $H = 4\pi^2 n_0^2 (dn/dc)^2/(N_A\lambda^4)$ and $q = (4\pi n_0/\lambda)\sin(\theta/2)$ with N_A, n_0, dn/dc, and λ being the Avogadro constant, the solvent refractive index, the specific refractive index increment of polymer in a given solvent, and the wavelength of laser light in a vacuum, respectively. In dynamic LLS, the intensity−intensity time correlation function $G^{(2)}(\tau)$ in the self-beating mode was measured. $G^{(2)}(\tau)$ has the form[23]

$$G^{(2)}(\tau) = A[1 + \beta|g^{(1)}(\tau)|^2] \tag{2}$$

with τ being the delay time, A the baseline, β a spatial coherence factor, and $g^{(1)}(\tau)$ the first-order normalized electric field correlation function, which is related to the normalized characteristic line width distribution function $G(\Gamma)$ by the Laplace integral equation.

$$g^{(1)}(\tau) = \int G(\Gamma)\exp(-\Gamma\tau)\,d\Gamma \tag{3}$$

By using a Laplace inversion program, CONTIN,[24] the normalized distribution function of the characteristic line width $G(\Gamma)$, the mean line width $\bar{\Gamma}$, and the variance $\mu_2/\bar{\Gamma}^2$ were obtained, with

$$\bar{\Gamma} = \int \Gamma G(\Gamma)\,d\Gamma \tag{4}$$

and

$$\mu_2 = \int (\Gamma - \bar{\Gamma})^2 G(\Gamma)\,d\Gamma \tag{5}$$

In the limit of q ($q \to 0$ and $qR_g < 1$), the mean characteristic line width $\bar{\Gamma}$ is related to the z-average translational diffusion coefficient D_z by the relation

$$\lim_{q\to 0} \bar{\Gamma} = D_z q^2 \tag{6}$$

The concentration effect can be represented by a second virial coefficient expansion

$$D_z = D_z^0(1 + k_d C) \tag{7}$$

where the superscript zero denotes the value at infinite dilution ($C \to 0$) and k_d is the diffusion second virial coefficient. At finite scattering angles, the characteristic line width could contain information on internal motions of the polymer as well as its translational motions. Equation 6 is no longer valid at $qR_g > 1$ but can be modified to yield

$$\bar{\Gamma}/q^2 \approx D_z(1 + f_c\langle R_g^2\rangle q^2) \tag{8}$$

where f_c is a dimensionless number and depends on chain structure, polydispersity, and solvent quality. If the translational diffusion coefficient D_z^0 is known, the hydrodynamic

radius R_h can be obtained from the Stokes−Einstein equation:

$$R_h = \frac{k_B T}{6\pi\eta D_z^0} \tag{9}$$

where k_B, T, and η are the Boltzmann constant, the absolute temperature, and the solvent viscosity, respectively.

Capillary Electrophoresis (CE). PDMA-*g*-PMMA solutions were prepared by dissolving the copolymer in methanol/1×TBE buffer (89 mM tris(hydroxymethyl)aminomethane, 89 mM boric acid, and 2 mM EDTA in deionized water) mixture at different ratios to the desired concentrations. The salt concentration in all solvent mixtures was kept constant. The pBR322/Hae III digest was purchased from Sigma-Aldrich Chemical Co. The DNA digest was diluted to 10 μg/mL by using deionized water. Separation was performed using the lab-built capillary electrophoresis system with laser-induced fluorescence detection.[25] 13 cm long fused-silica capillaries (Polymicro Technologies, Phoenix, AZ) with I.D./O.D. of 75/365 μm were used in our experiments. A detection window (2 mm) was opened at 3 cm from the anode end by stripping off the polyimide coating with a razor blade. The capillary was flushed with 1 M HCl for 10 min. Both cathode and anode reservoirs (1.6 mL volume) were filled with the same buffer as used for preparing the polymer solution and 3 μg/mL ethidium bromide. The separation medium was filled into the capillary tubing by using a gastight syringe. Before each electrophoresis run, the capillary column was conditioned under an electric field strength of 300 V/cm to introduce the fluorescence dye into the separation medium and to stabilize the current. The DNA sample was electrokinetically injected into the capillary at an electric field strength of 50 V/cm for 3 s. Electrophoresis was conducted under an applied electric field strength of 150 V/cm. For the free solution mobility measurements, a 3/6 cm (effective/total) long capillary column was used which was coated by 0.1 wt % PDMA solution with a molecular weight of 470K Da. DNA was injected into the capillary at 50 V/cm for 3 s. Electrophoresis was operated at 125 V/cm.

Results and Discussion

The weight-average molecular weight of the graft copolymer PDMA-*g*-PMMA was measured by conventional static laser light scattering. The graft copolymer used here had two components PDMA and PMMA. However, its overall refractive index could be approximated as that of a homopolymer because the specific refractive index increments for PDMA and PMMA chains (0.144 mL/g) were very close to each other in methanol solutions, and the PMMA fraction in the copolymer was relatively small.[22,26] Figure 1a shows a Zimm plot of PDMA-*g*-PMMA graft copolymer in methanol solution at 25 °C. The molecular weight of the graft copolymer was determined from the Zimm plot to be 2.37×10^6 g/mol, and it had a radius of gyration of 83.8 nm. Figure 1b shows the concentration dependence of the translational diffusion coefficient measured by dynamic laser light scattering. According to the Stokes−Einstein equation, the hydrodynamic radius R_h of PDMA-*g*-PMMA had a value of 52.4 nm. The R_g/R_h ratio of this graft copolymer in methanol solution was 1.6, similar to that of a linear homopolymer in a good solvent, indicating that the PDMA-*g*-PMMA copolymer in methanol had a random coil conformation.

We used the macromonomer vinyl-PMMA as the side chain of the graft copolymer. The molecular weight was known to be about 5 kg/mol (weight-average). Based on the feed ratio, the fraction of the side chains should be very small in the graft copolymer. The amount of PMMA in the PDMA-*g*-PMMA copolymer could be estimated by using ^{1}H nuclear magnetic resonance spectroscopy

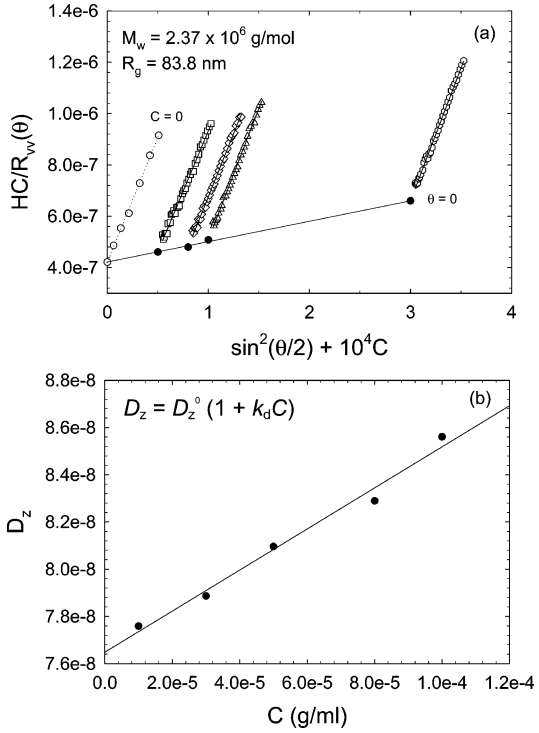

Figure 1. PDMA-*g*-PMMA copolymer in methanol solution at 25 °C: (a) Zimm plot and (b) translational diffusion coefficient vs concentration measured by dynamic laser light scattering.

(data not shown here). From the integral areas of methyl protons in PDMA and methyl group attached on the methine in PMMA, a molar ratio of 50 of DMA/MMA was obtained, which corresponded to a total PMMA content of about 2.0 wt % in the PDMA-*g*-PMMA copolymer. The averaged number of side chains in the graft copolymer molecule was 9.4, indicating that there was one PMMA side chain for about every 2500 repeating units on the backbone chain.

To investigate the association behavior of PDMA-*g*-PMMA graft copolymer in methanol/1×TBE mixture, we first dissolved the graft copolymer in pure methanol dispersing the graft copolymer chains. The polymer solution was filled in a dust-free light scattering cell for light scattering experiments. After having measured the solution behavior by light scattering, we added the 1×TBE buffer into the cell to the desired TBE fraction, vortexed the solution, waited for 60 min to equilibrate the solution, and then measured both static and dynamic light scattering. Additional amounts of 1×TBE buffer were added, mixed, and equilibrated before each set of light scattering measurements. The procedure was repeated until the TBE volume fraction reached 0.5 of the solvent mixture. The TBE buffer was filtered by using 0.1 μm pore size Millipore filters before use. The values of refractive indices for methanol (1.326) and TBE buffer (1.334) were close. So the composition dependence for the specific refractive index increment of this copolymer in methanol/TBE mixture could be ignored.[22] All values including the weight-average molecular weight, the radius of gyration, and the hydrodynamic radius were referred to as apparent values without extrapolation to the infinite dilution limit. The association behavior could be affected by the solution concentration. However, the error introduced should be acceptable for qualitative discussions. It is noted that in a mixed solvent preferential adsorption may occur,

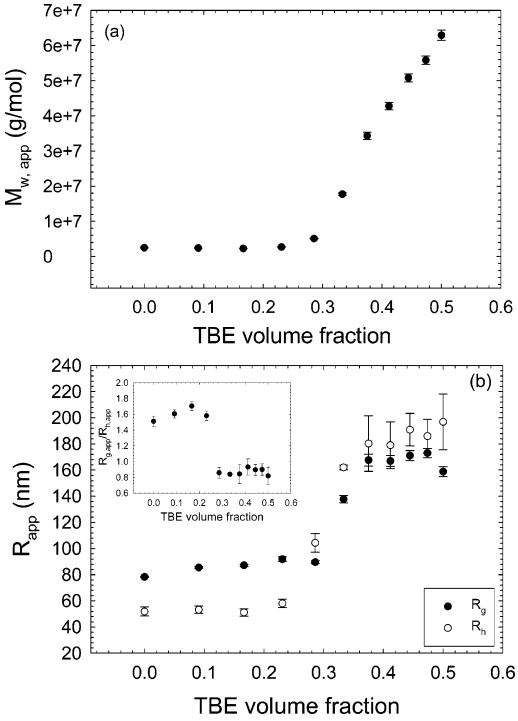

Figure 2. $M_{w,app}$ (a), $R_{g,app}$, and $R_{h,app}$ (b) as a function of the TBE buffer volume fraction of methanol/TBE mixed solvent for PDMA-*g*-PMMA solutions prepared by diluting 5×10^{-5} g/mL stock copolymer solution in pure methanol. The inset in (b) shows the $R_{g,app}/R_{h,app}$ ratio dependence of TBE volume fraction.

and the solvent−solute interactions change with the solvent composition, together with changes in solvent−solvent interactions. Thus, a more critical experiment requires dialysis to ensure the corresponding equilibration in the chemical potential. We have not done so in this set of experiments because the light scattering data are, in essence, used to discuss the qualitative nature of the system. Quantitative analysis is not warranted for the conclusions we seek**.** Figure 2a,b shows the $M_{w,app}$, $R_{g,app}$, and $R_{h,app}$ dependence of the TBE buffer volume fraction of methanol/TBE mixed solvent for PDMA-*g*-PMMA solutions prepared by diluting 5×10^{-5} g/mL stock solution in pure methanol. Before the TBE volume fraction reached 0.3, $M_{w,app}$, $R_{g,app}$, and $R_{h,app}$ values did not change much and were almost constant. When the TBE volume fraction was above 0.3, there was a sudden change on all these quantities. The transition region was very narrow. The radius of gyration and the hydrodynamic radius were almost constant (Figure 2b), irrespective of the solvent quality once the association started to occur. The aggregates had an average association number of the order of 20 at a TBE volume fraction value of about 0.4. The starting solution used here had a concentration well below the overlap concentration (about 1.6×10^{-3} g/mol as calculated by using the equation $C^* \sim 3M_w/4\pi R_g^3 N_A$). Before adding the TBE buffer to the solution, the methanol was a good solvent to both components of the graft copolymer, and the copolymer adopted a random chain conformation. With the addition of TBE buffer to the solution, the solvent quality decreased for PMMA. The hydrophobic part, i.e., PMMA, of the graft copolymer tended to aggregate together in order to avoid contacts with the TBE buffer. When the TBE buffer fraction was below 0.3, no intramolecular association was observed because there was little change in the molecular size. After the

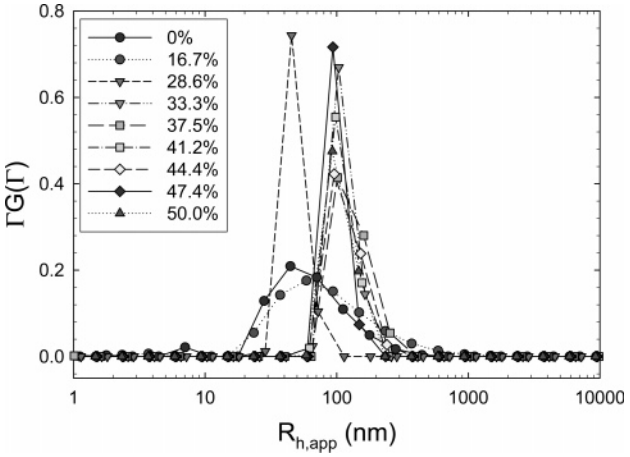

Figure 3. TBE buffer volume fraction dependence of hydrodynamic radius distribution of PDMA-*g*-PMMA copolymer solutions at $\theta = 30°$ and $C_{start} = 5 \times 10^{-5}$ g/mL.

TBE volume fraction exceeded 0.3, intermolecular aggregation began to form. On average, almost 8 molecules associated together to form an aggregate at a TBE volume fraction of 0.3. By further adding the TBE buffer, more and more molecules were associated together, with increasing molecular weight of the aggregates, while the particles size remained almost constant. This observation implies that the aggregates became denser with increasing TBE buffer content. We did not investigate the polymer concentration effect on the aggregation behavior because there was little difference in the aggregation behavior for the solutions at different concentrations.[22] The only change was the solvent composition at the onset of the aggregation.

The ratio of radius of gyration to hydrodynamic radius (R_g/R_h) is an indication of the molecular chain conformation in dilute solution. It is well-known that for a random coil in a good solvent $\langle R_g\rangle/\langle R_h\rangle \sim 1.5$, while for a uniform solid sphere, $\langle R_g\rangle/\langle R_h\rangle \sim 0.774$.[27] To evaluate the graft copolymer PDMA-*g*-PMMA chain conformation in dilute solution, a ratio of apparent radius of gyration to apparent hydrodynamic radius was determined. The inset in Figure 2b shows the $R_{g,app}/R_{h,app}$ ratio dependence of TBE volume fraction in the mixed solvent for PDMA-*g*-PMMA solutions at $C = 5 \times 10^{-5}$ g/mL. Before the TBE volume fraction was 0.3, the solvent quality was relatively good for the graft copolymer PDMA-*g*-PMMA. The $R_{g,app}/R_{h,app}$ ratios at all compositions were around 1.6, indicating an expanded random coil conformation for the graft copolymers in solution. After the TBE volume fraction was greater than 0.3, the ratio suddenly jumped down to the value of about 1.1. This decrease of the $R_{g,app}/R_{h,app}$ ratio indicated that the polymer chains shrank and got condensed due to the decrease in solvent quality for the PMMA part of the graft copolymer.

Figure 3 shows the dependence of the apparent hydrodynamic radius ($R_{h,app}$) distribution of PDMA-*g*-PMMA graft copolymer on TBE volume fraction in methanol/TBE mixed solvent at $C = 5 \times 10^{-5}$ g/mL and $\theta = 30°$. With an increase in the TBE buffer volume fraction, the size distribution became narrower with the average R_h value remained essentially constant (∼52 nm) before the TBE volume fraction reached 0.3. At volume fractions greater than 0.3, the hydrodynamic radius (with a narrow size distribution) jumped to larger values (∼185 nm). The observed results indicated a

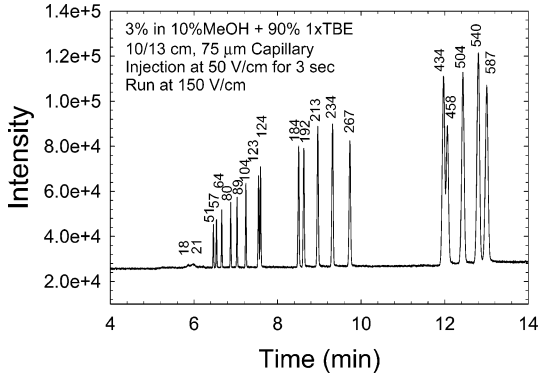

Figure 4. Electropherogram of pBR322/Hae III digest by using 3% (w/v) PDMA-*g*-PMMA copolymer in 10% methanol + 90% TBE mixture solution as a separation medium at room temperature. The 20 fragments range from 18 to 587 bp. Conditions: l (length to detector) = 10 cm, L (column length) = 13 cm, E (voltage) = 150 V/cm, capillary I.D. = 75 μm, O.D. = 360 μm, 1×TBE buffer, electrokinetic injection at 50 V/cm for 3 s.

solvent quality induced aggregation behavior occurring for the PDMA-*g*-PMMA graft copolymer in methanol/TBE mixed solvent. The graft copolymer had an expanded random coil conformation in methanol (a good solvent). The addition of TBE buffer made the solvent quality poorer and forced the hydrophobic PMMA part of the copolymer to aggregate together to form the aggregates with a narrower size distribution.

The intra- and intermolecular associations of the side chains provided the network with certain "fixed" crosslinks at concentrations above the overlap concentration. The pore size could become more stable because such aggregation behavior should be more permanent than that of linear chain entanglements. Furthermore, these interlocking points could link different molecules together (intermolecular association) and effectively increase the apparent polymer molecular weight, a desirable specification for large DNA fragment separations. Thus, such an aggregated graft copolymer PDMA-*g*-PMMA could be used as a high-performance separation medium for DNA separation. To prove the high sieving ability of PDMA-*g*-PMMA graft copolymer as a DNA separation medium, DNA separation was carried out in polymer solutions at a relatively high concentration of 3% (w/v). The DNA sample, pBR322/HaeIII digest containing 22 fragments ranging from 8 to 587 bp including 123 and 124 bp with one base difference, was used for the test on DNA separation by capillary electrophoresis. Figure 4 shows the electropherogram of pBR322/Hae III digest by using 3% (w/v) PDMA-*g*-PMMA copolymer in 10% methanol + 90% TBE (by volume) mixture solution as a separation medium at room temperature. All fragments larger than 22 bp in the pBR322/Hae III digest were clearly separated within 13 min with 10/13 cm (effective/total) length capillary at 150 V/cm. The doublet fragments of 123/124 bp were almost baseline separated. In comparison with the separation result by using another separation medium, graft copolymer PNIPAM-*g*-PEO developed in our lab,[15] it has a comparable resolution but much less migration time. Table 2 shows the comparison of pBR322/HaeIII digest separation by CE using different separation media at different separation conditions. Compared with linear polyacrylamide, the separation medium with the best sieving ability, our polymer showed similar resolution, but without coating the capillary wall in advance.

Table 2. Comparison of pBR322/Hae III Digest Separation by Different Separation Media

media name	mol wt (Da)	concn % (g/mL)	finish time (min)	ref
LPA	2.2×10^6	2.5	11.7	28
LPA + glycerol	2.2×10^6	2.5	38.5	28
PEO	8×10^6	2	11.7	28
PEO + glycerol	8×10^6	2	34.1	28
LPA	700K−1M	6	72	29
PDMA + clay	100K	5	13	30
PDMA + PDMA	100K + 1M	1 + 2	13	30
PNIPAM + PEO	6.4×10^7	10	39.2	15
PNIPAM + PEO	>10 M	8	12.3	31
$B_{10}E_{271}B_{10}$ + $B_6E_{46}B_6$	13K + 2.8K	4 + 5	20.4	2
PVP + PAM (IPN)	1M + 400K	2 + 1	6.5	32
PVP + PDMA (IPN)	1M + ?	4 + 4	20.8	19
PAEG	240K	7.5	30	33
PDMA-*g*-PMMA	2.37×10^6	3	13	

It should be noted that the molecular weight, the grafting density, and the length of side chain of our copolymers were not optimized. If all conditions were optimized, this copolymer should be able to exceed its performance beyond the best-known sieving ability separation medium for dsDNA separations over the size range of our investigation.

On the basis of the scattering experiments, the graft copolymer PDMA-*g*-PMMA began to aggregate in methanol/TBE mixed solvent when the TBE volume fraction was above 0.3. Polymer solutions at a certain concentration with the solvent composition beyond that transition point should, in principle, be suitable as DNA separation media. The association strength of the grafted chains should depend on the solvent composition. On the basis of the pore size separation mechanism, small size DNA fragments should obtain better separation resolution at higher TBE buffer fraction. Figure 5A−D shows the electropherograms of pBR322/Hae III digest by using 3% (w/v) PDMA-*g*-PMMA copolymer in methanol/TBE mixed solvent at different methanol compositions as the separation media at room temperature. Increasing the methanol content in the mixed solvent (from (A) to (D)) resulted in the following effects: (1) It destroyed the separation of the 123/124 bp doublet fragment. (2) The separation resolution for the larger DNA fragments improved. (3) It prolonged the separation time (time almost doubled). It could be concluded from Figure 5 that the lower the methanol content in the polymer solution and running buffer, the better the separation resolution for the smaller DNA fragments could achieve. On the other side, the higher the methanol content, the better the resolution for the larger DNA fragments. If the PDMA-*g*-PMMA copolymer solution in pure TBE buffer was used as a separation medium, it would have the shortest running time with the best resolution for the smaller DNA fragments. The PDMA-*g*-PMMA copolymer was difficult to dissolve in the pure TBE buffer. The solution was prepared by first dissolving the polymer in 90% TBE and 10% methanol mixed solvent, and then the methanol component was carefully removed by evaporation which was monitored by weight. Figure 6 shows the separation of bPR322/HaeIII digest by using 3% (w/v) PDMA-*g*-PMMA copolymer in pure TBE buffer as a separation medium. It is in good agreement with the prediction. All fragments were separated within 10 min, and 123/124 bp was baseline separated. It should be noted that the first detectable peaks for fragments 18 and 21 bp long were clearly shown in the electropherogram. Better resolution for the

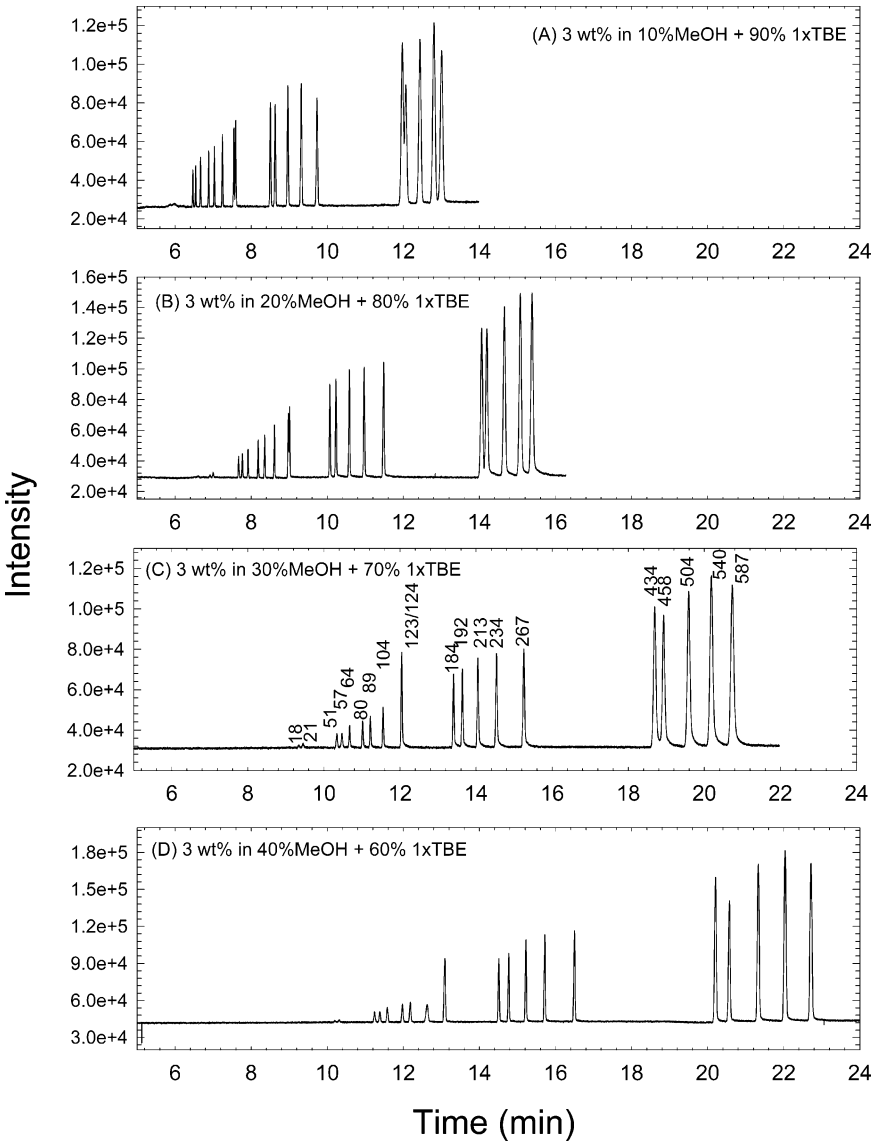

Figure 5. Electropherograms of pBR322/Hae III digest by using 3% (w/v) PDMA-*g*-PMMA copolymer in methanol/TBE mixed solvent at different TBE compositions as the separation medium at room temperature. Conditions same as in Figure 1.

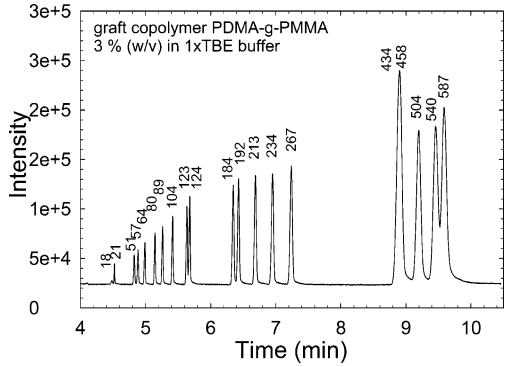

Figure 6. Electropherogram of pBR322/Hae III digest by using 3% (w/v) PDMA-*g*-PMMA graft copolymer in 1×TBE buffer solution without methanol as a separation medium at room temperature. Conditions same as in Figure 1.

smaller DNA fragments was accompanied by a decrease in the larger DNA fragments separation resolution. Fragments 434 and 458 bp were merged into one peak, and 540 and 587 bp fragments were poorly separated.

The free solution electrophoretic mobility of polyelectrolytes has been rationalized in terms of their size, effective charge density, and viscosity of the solvent. In capillary electrophoresis (CE), the most commonly used model is the Hückel equation:[34]

$$\mu_0 = \frac{q}{6\pi\eta R} \tag{10}$$

where μ_0 is the free solution mobility, η is the solvent viscosity, and q (different meaning from q in eq 1) and R are the polyion's charge and radius, respectively. To investigate the methanol effect on the double-stranded DNA separation, capillary zone electrophoresis (CAE) and dynamic light scattering were employed to measure the free solution mobility and hydrodynamic radius (R_h) of DNA. Figure 7 shows the effect of methanol volume fraction in mixed solvent on the DNA free solution mobility. The electrophoretic mobility of DNA was found to be 3.08×10^{-4} cm^2 V^{-1} s^{-1} in TBE buffer. By adding methanol, the free solution mobility decreased to 1.27×10^{-4} cm^2 V^{-1} s^{-1} when the methanol volume fraction was 0.3. The inset in Figure 7 shows the current change with methanol volume fraction during capillary zone electrophoresis. At fixed condition, the separation speed is proportional to the current. Figure 7 explains the

Table 3. Effective Charge Density Change of DNA at Different Methanol Content

methanol volume fraction (%)	free solution mobility (10^4 cm^2 V^{-1} s^{-1})	solvent viscosity (cP)	apparent hydrodynamic radius (nm)	percent of remaining effective charge density (%)
0	3.08	0.89	76.2	100
10	2.42	1.07	74.8	92.6
20	1.73	1.26	59.0	61.4
30	1.27	1.41	43.7	37.6

speed retardation by methanol from the view of free solution mobility. The other two factors, solvent viscosity and DNA radius, also affect the separation speed. A representative apparent hydrodynamic radius ($R_{h,app}$) distribution of pCMVβ plasmid DNA is shown in Figure 8. At 25 °C, the supercoiled double-stranded DNA in 1×TBE buffer had a wide size distribution with an average $R_{h,app}$ of about 76.2 nm. This kind of DNA has the same molecular weight but different conformations in solution. When methanol was added, the average $R_{h,app}$ was decreased and the size distribution became narrower, suggesting that DNA changed their conformations during the addition of methanol. The effective charge density could be calculated out by eq 10. Table 3 shows the effective charge density change at different methanol composition. The effective charge density directly affects the separation speed of DNA fragments. The retardation of the separation speed is due to the reduced effective charge density when methanol was added into the TBE buffer.

In capillary electrophoresis the DNA fragments with size larger than the mesh size migrate through the polymer network by reptation with stretching. DNA separation is dependent on its conformation. Karger et al. even found that two fragments with the same length could be separated if there were a conformation difference between the two species.[29] Liang et al. have investigated the effect of adding glycerol to the running buffer on DNA separation using LPA or PEO as the separation medium.[28] The results after adding the glycerol to the running buffer was the same as ours. They partially attributed the improvement for the larger DNA fragments separation to the ability of glycerol to induce a chain conformation change in DNA. The increased electrostatic interactions between phosphate groups induced by the presence of glycerol increased the DNA contour length and reduce the effective charges over weight ratio and hence improved the separation resolution for the larger DNA fragments. DLS data (Figure 8) clearly shows the DNA conformation changes. These conformation changes resulted in the improvement of larger DNA fragments separation.

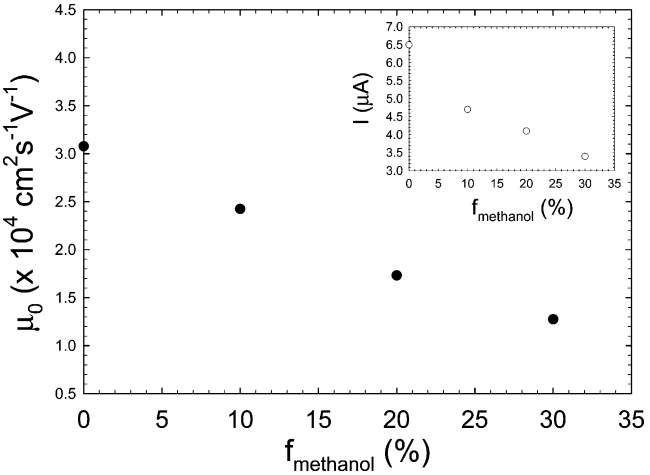

Figure 7. Free solution mobility of pCMVβ plasmid DNA at different methanol content in the mixed solvent. Conditions same as in Figure 1, except capillary effective/total length = 3/6 cm and E (voltage) = 125 V/cm.

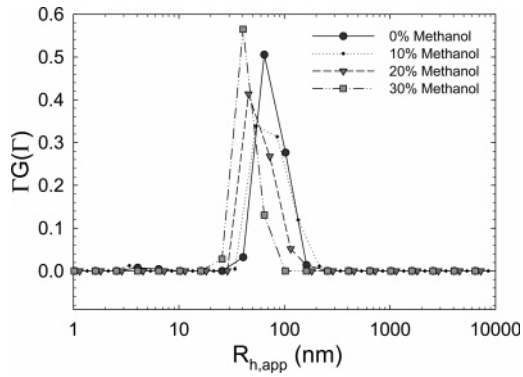

Figure 8. pCMVβ plasmid DNA apparent hydrodynamic radius distribution at different methanol composition (volume fraction) in the mixed solvent. The plasmid DNA sample was diluted to 1×10^{-5} g/mL and DLS was measured at 30°.

Conclusions

The association behavior of high molecular weight graft copolymer PDMA-*g*-PMMA with low graft density has been investigated by laser light scattering. The copolymer could undergo a very sharp solvent quality induced aggregation transition. At low TBE volume fraction, the copolymer chains adopted an expanded random coil conformation in dilute solutions. When the TBE volume fraction reached 0.3, side-chain association and intermolecular aggregation began to occur. At high copolymer concentrations, the associated side chains could act as cross-linking points. These interlocking points effectively increased the polymer apparent molecular weight and stabilized the pore size of the polymer (quasi-)network by preventing the backbone chains in sliding away from one another. These features offered such materials a better sieving ability for DNA separations. pBR322/Hae III digest was successfully separated with good separation resolution and speed when using this type of graft copolymer as a viable separation medium. The addition of methanol into TBE buffer decreased the effective charge density and hydrodynamic radius of DNA. The separation retardation and resolution improvement for the larger DNA fragments were due to the change of effective charge density and conformation of DNA.

Acknowledgment. B.C. gratefully acknowledges the support of this work by the National Human Genome Research Institute (NIH 2R01HG01386-09) and the National Science Foundation (DMR-9984102).

References and Notes

(1) Wu, C.; Liu, T.; Chu, B. *Macromolecules* **1997**, *30*, 4574−4583.
(2) Liu, T.; Liang, D.; Song, L.; Nace, V. M.; Chu, B. *Electrophoresis* **2001**, *22*, 449−458.
(3) Park, S.; Healy, K. E. *Bioconjugate Chem.* **2003**, *14*, 311−319.
(4) Xu, R.; Winnik, M. A. *Macromolecules* **1991**, *24*, 87−93.

(5) Zhou, Z.; Chu, B.; Peiffer, D. G. *Macromolecules* **1993**, *26*, 1876−1883.
(6) Paul, C. W.; Cotts, P. M. *Macromolecules* **1987**, *20*, 1986−1991.
(7) Balsara, N. P.; Tirrell, M.; Lodge, T. P. *Macromolecules* **1991**, *24*, 1975−1986.
(8) Kikuchi, A.; Nose, T. *Macromolecules* **1996**, *29*, 6770−6777.
(9) Kikuchi, A.; Nose, T. *Polymer* **1996**, *37*, 5889−5896.
(10) Heiger, D. N.; Cohen, A. S.; Karger, B. L. *J. Chromatogr. A* **1990**, *516*, 33−48.
(11) Schwartz, H. E.; Ulfelder, K.; Sunzeri, F. J.; Busch, M. P.; Brownlee, R. G. *J. Chromatogr. A* **1991**, *559*, 267−283.
(12) Paulus, A.; Ohms, J. I. *J. Chromatogr. A* **1990**, *507*, 113−123.
(13) Drossman, H.; Luckey, J. A.; Kostichka, A. J.; D'Cunha, J.; Smith, L. M. *Anal. Chem.* **1990**, *62*, 900−903.
(14) Song, L.; Liang, D.; Kielescawa, J.; Liang, J.; Tjoe, E.; Fang, D.; Chu, B. *Electrophoresis* **2001**, *22*, 729−736.
(15) Liang, D.; Zhou, S.; Song, L.; Zaitsev, V. S.; Chu, B. *Macromolecules* **1999**, *32*, 6326−6332.
(16) Sudor, J.; Barbier, V.; Thirot, S.; Godfrin, D.; Hourdet, D.; Millequant, M.; Blanchard, J.; Viovy, J. L. *Electrophoresis* **2001**, *22*, 720−728.
(17) Menchen, S.; Johnson, B.; Winnik, M. A.; Xu, B. *Electrophoresis* **1996**, *17*, 1451−1459.
(18) Menchen, S.; Johnson, B.; Winnik, M. A.; Xu, B. *Chem. Mater.* **1996**, *8*, 2205−2208.
(19) Wang, Y.; Liang, D.; Hao, J.; Fang, D.; Chu, B. *Electrophoresis* **2002**, *23*, 1460−1466.
(20) Grossman, P. D.; Soane, D. S. *Biopolymer* **1991**, *31*, 1221−1228.
(21) Bae, Y. C.; Soane, D. S. *J. Chromatogr. A* **1993**, *652*, 17−22.
(22) Itakura, M.; Inomata, K.; Nose, T. *Polymer* **2001**, *42*, 9261−9268.
(23) Chu, B. *Laser Light Scattering*, 2nd ed.; Academic Press: New York, 1991.
(24) Provencher, S. W. *Makromol. Chem.* **1979**, *180*, 201.
(25) Song, L.; Liang, D.; Fang, D.; Chu, B. *Electrophoresis* **2001**, *22*, 1987−1996.
(26) Benoit, H.; Floelich, D. I.; Huglin, M. B. *Light Scattering from Polymer Solution*; Academic Press: New York, 1972.
(27) Zhang, G.; Winnik, F. M.; Wu, C. *Phys. Rev. Lett.* **2003**, *90*, 035506-1.
(28) Liang, D.; Song, L.; Chen, Z.; Chu, B. *J. Chromatogr. A* **2001**, *931*, 163−173.
(29) Pariat, Y. F.; Berka, J.; Heiger, D. N.; Schmitt, T.; Vilenchik, M.; Cohen, A. S.; Foret, F.; Karger, B. L. *J. Chromatogr. A* **1993**, *652*, 57−66.
(30) Liang, D.; Song, L.; Chen, Z.; Chu, B. *Electrophoresis* **2001**, *22*, 1997−2003.
(31) Liang, D.; Song, L.; Zhou, S.; Zaitsev, V. S.; Chu, B. *Electrophoresis* **1999**, *20*, 2856−2863.
(32) Song, L.; Liu, T.; Liang, D.; Fang, D.; Chu, B. *Electrophoresis* **2001**, *22*, 3688−3698.
(33) Chiari, M.; Riva, S.; Gelain, A.; Vitale, A.; Turati, E. *J. Chromatogr. A* **1997**, *781*, 347−355.
(34) Roy, K. I.; Lucy, C. A. *Electrophoresis* **2003**, *24*, 370−379.

MA0490193